Origin of Link Gain Fluctuations in Analog Radio over Single-Mode Fiber Systems

Simone Rusticelli[b], Federico Perini[a], Jader Monari[a], Giovanni Tartarini[b,1]

[a] *Institute of Radio Astronomy, National Institute for Astrophysics, Via Fiorentina 3513, 40059 Medicina, Italia*
[b] *Department of Electrical and Information Engineering, University of Bologna, Viale Risorgimento 2, 40136 Bologna, Italia.*

Abstract

In analog Radio over Fiber systems based on single mode fibers, the possible presence of unexpected fluctuating behaviors of amplitude and phase of the received radiofrequency signal in front of monotonic environmental temperature variations, is analyzed experimentally and simulated theoretically. The possibility to understand all the aspects of this behavior allows to keep it in the right account, particularly when these systems have to be realized with stringent requirements in terms of cost and performance.

Keywords: Radio over Fiber, Radioastronomy, RF gain, RF phase, DFB, VCSEL

1. INTRODUCTION

Among the techniques utilized within the world of Microwave Photonics [1], Radio over Fiber (RoF) plays a primary role. Systems which exploit this technique can be found in telecommunications, to realize capillary distribution of the mobile signals in crowded or non-line-of-sight environments [2], in meteorology and defense, for radar antenna remoting [3], in measurement and monitoring applications [4][5] and in radioastronomy [6][7], where the optical fiber as a transmitting medium guarantees to the radiofrequency (RF) signal low attenuation and immunity to electromagnetic interference. In all the above mentioned applications, when the RoF systems are not located in closed, environmentally controlled placements, the influence of variable quantities, temperature *in primis*, on the system performances must be taken into account. Technical information given by the producers of optical components, include to this purpose the dependence on temperature variations of quantities like the laser current-power conversion efficiency, the emission wavelength, the photiodiode responsivity, etc. Thanks to the knowledge of these dependencies, an appropriate design of analog RoF links can be realized, where substantially monotonic variations of the environmental temperature lead to predictable monotonic variations of quantities like the received optical power, or the RF gain of the RoF link.

Even little deviations from these expected monotonic behaviors can be of primary detrimental importance in applications where it is possible that RF signals with very low power levels have to be detected. This can be the case of all the fields cited above, in particular those where RoF links operate within sensing apparatus (radar antennas, monitoring systems, radioastronomic stations, and so on).

In this paper we will show that one of the possible causes which can determine undesired fluctuations of RoF links characteristic quantities, is the combined presence of:

- optical back reflection of the laser emitted power in the region where coupling with the input section of the optical fiber is realized;
- variations in the laser operating temperature.

The problem of back reflection of laser light in optical fiber systems is known, and solutions have already been proposed, based mainly on the introduction of an optical isolator in the region where the laser to fiber coupling is performed. In this way, the level of optical backreflection is reduced to levels which can be regarded as negligible for many of

[1] Corresponding Author Tel: +390512093051, email: giovanni.tartarini@unibo.it

the laser's envisaged applications [8].

The effects of temperature variations on the laser characteristics (emitted optical power, value of the threshold current, optical emission wavelength, etc.) are also well known, and, if necessary, can be reduced in their impact, endowing the laser with appropriate thermostabilization equipments [9].

However, there are practical situations where both problems have to be taken into account. In the case of RoF systems, this can happen when, searching for a compromise between high performance and low cost, laser sources are utilized which are not optimized for the transmission of radio signals, having been originally designed for digital applications, and/or which lack optical isolators and/or thermostabilization equipments.

Having the possibility to model and make the RoF system response predictable and/or controllable is therefore important in these practical situations. For example, in the area of Radioastronomy, this is the case of the "Square Kilometre Array" project (SKA) [10], or of the technological upgrade of the large antenna dishes for Very Long Baseline Interferometric (VLBI) applications, which both must exploit a very high number of analog RoF links to transport the signal received by the antennas.

In this paper, an analysis will be performed of RoF links where the laser transmitters exhibit both a degree of optical backreflection and a dependence on the operating temperature of the optical emission wavelength. A theoretical model which allows to put into evidence the combined influence of these characteristics on the system's behavior and simulate their consequent detrimental effects will be presented, together with some experimental results confirming the correctness of the approach. Some general guidelines will then be identified to keep the impact of the problem adequately into account, and finally conclusions will be drawn.

2. OBSERVED BEHAVIOR AND THEORETICAL MODEL DEVELOPED

2.1. Identification of the problem

The first experimental evidence of the phenomenon described in this work came during the test of analog RoF links utilized for the receiver chain of the BEST (Basic Element for SKA Training) system, which is one of the three technological demonstrators realized in the frame of the FP6-SKADS (SKADesign Study) project. BEST is based on the re-instrumentation of part of the Northern Cross Radio Telescope located in Medicina, Italy [11][12].

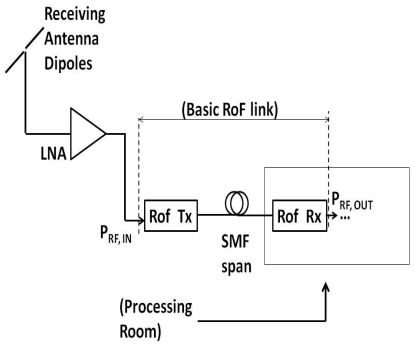

Figure 1: Configuration of the receiver part of the Northern Cross Radio Telescope equipped with analog RoF links.

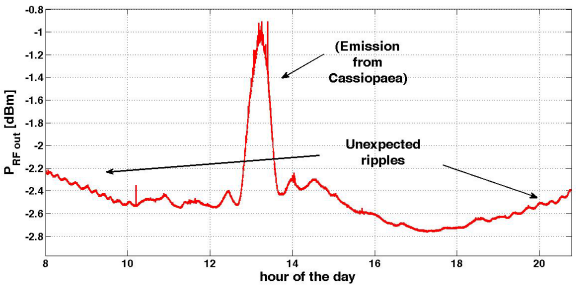

Figure 2: Typical behavior of the RF power received by the RoF link of Fig. 1 in a span of time ranging from morning to evening.

The links considered (see Fig. 1) were composed by a RoF Tx based on a DFB operating at a wavelength $\lambda = 1310nm$, directly modulated by a Low Noise RF Amplifier (LNA) and placed immediately after a subset of the receiving antenna dipoles. The fiber optic span was composed by a few hundred meters of G-652 SMF, connecting the RoF Tx to the central processing room where the RoF Rx was placed, based on a PIN photodiode (PD). The operating RF frequency was $f_{RF} = 408 \pm 8$ MHz. With reference to these links, in front of monotonic decreasing or increasing temperature changes, slow modulating ripples appeared in the behavior of the received RF power, which were superimposed to its expected, and more manageable, monotonic variation (see Fig. 2).

This behavior determines a reduction of the sensitivity of the instrument. Indeed, in single-antenna observations, the sensitivity is inversely proportional to the ratio $\frac{\delta G}{G}$ (where G is the RF gain of the receiver chain). Moreover, in observations with arrays, where a combination of the antennas is performed to generate different beams, fluctuations of the gain bring to pointing errors and to a reduction of the quality of the beams themselves (like the growth of secondary lobes). Given the extremely weak nature of the signals that have to be determined with the radiotelescopes (of the order of $10^{-26} W/m^2/Hz$), even fluctuations that are negligible in other applications can sensibly reduce the quality of the observations. The fact that these behaviors have been observed in RoF links based on Single Mode Fibers (SMF) allowed to exclude the phenomenon of modal noise from the possible causes, since the undesired fluctuations due to Modal Noise take place only in RoF links based on MMF [13] [14].

From subsequent laboratory experiments based on the use of various RoF transmitters (Tx's), RoF receivers (Rx's), and fiber span lengths, it was found that the phenomenon depends on the characteristics of the RoF Tx. A further preliminary test consisted in the extraction and utilization of the only DFB laser from one the RoF Tx's. This operation was done in order to rule out possible influences on the investigated behavior from the components of the RoF TX, like the matching and/or the optical power control circuit. The fluctuations of the RF gain of the link were indeed still observed, indicating that the origin of the behavior is due to the laser itself. Moreover, from subsequent measurements performed with the help of polarization filter, polarization controller, and polarization maintaining fiber, it was excluded that the behavior was related to a sort of modal noise between the two polarizations of the LP_{01} mode.

It was then concluded that the origin of this behavior must be ascribed to undesired backreflections which take place in the region between laser and fiber input section. Through a simple electromagnetic model, this assumption will now be formalized, and some characteristics of the phenomenon will be put into evidence.

2.2. Mathematical model

A basic RoF link is considered, like the one schematized in Fig. 1, where a Tx, based on a laser directly modulated in intensity with an RF sinusoidal tone, emits an optical field which is coupled to an SMF span. After propagation in the fiber, the field is then converted into an electrical current using the direct detection (DD) technique by a RoF Rx based on a PIN photodiode. An undesired reflection is assumed to be experienced by the electrical field in a portion L (no more than a few millimeters long) of the optical path between the laser output section and the SMF input section. This double reflection can take place for example between the fiber pigtail input section and the laser output section, if nothing is present between them, or it can involve also other components possibly present between them, like a collimating lens. The field coupled into the SMF results then to be the sum of the field that would have been coupled without the undesired reflection, plus a retarded version of the field itself, which has undergone a double reflection with coefficients r_1 and r_2 , as well as a delay $\tau = \frac{2L}{c}$, where c is the speed of light, due to the additional back and forth distance of 2L covered in air. The electrical field at the output section of a span of optical fiber of length L_f can then be represented as:

$$\begin{aligned}
&\overline{E}_{out}(t, z = L_f) = \\
&= E_0 \overline{e}(x, y) e^{j(2\pi f_0 t - \beta L_f)} \cdot \\
&\cdot \Big(\{1 + m_I \cos[2\pi f_{RF}(t - \tau_0)]\}^{\frac{1}{2}} \cdot \\
&e^{j m_P \sin[2\pi f_{RF}(t-\tau_0)]} + \\
&+ r_1 r_2 e^{2jkL} \cdot \\
&\{1 + m_I \cos[2\pi f_{RF}(t - \tau_0 - \tau)]\}^{\frac{1}{2}} \cdot \\
&\cdot e^{j m_P \sin[2\pi f_{RF}(t-\tau_0-\tau)]} \Big)
\end{aligned} \tag{1}$$

where $\overline{e}(x, y)$ is the normalized field of the fundamental mode propagating in the fiber, E_0 is its amplitude, while β is its phase constant. The amplitude E_0 is proportional to the square root of the optical power $P_0 = \eta_0(I_{bias} - I_{th})$, where η_0 is the current-power conversion efficiency of the laser at DC, while I_{bias} and I_{th} are respectively the laser bias and threshold currents. The quantity f_0 is the optical carrier's frequency and $k = \frac{2\pi}{\lambda}$ is the wavenumber in free space. Moreover, $m_P = \frac{(K_f I_{RF})}{f_{RF}}$ is the phase modulation index of the optical wave determined by the frequency chirp of the laser, where K_f is its adiabatic chirp factor, I_{RF} is the amplitude of the modulating RF current, and

f_{RF} is its frequency, which can present values ranging from some hundred MHz to a few GHz. With m_I the optical modulation index (often referred in literature also with the acronym OMI) is indicated, defined as $m_I = \frac{(\eta_{RF} I_{RF})}{\eta_0 (I_{bias} - I_{th})}$, where η_{RF} is the current-power conversion efficiency of the laser at frequency f_c. The quantities τ_0 and τ are respectively the group delay caused by the propagation in the fiber span and the additional group delay of the portion of the original field which has undergone a double reflection before being coupled to the SMF. No phase noise is taken into account, since a highly coherent laser source is considered, with a line-width below 10 MHz. The received current is proportional to the optical power received on the PD surface S_{PD} (a Responsivity R=1 is assumed), namely:

$$
\begin{aligned}
& I_{out}(t, z = L_f) = \\
& = \int_{S_{PD}} |E_{out}(t, z = L_f)|^2 \, dS = \\
& = |E_0|^2 \left(\{1 + m_I \cos [2\pi f_{RF}(t - \tau_0)]\} + \right. \\
& + (r_1 r_2)^2 \{1 + \\
& + m_I \cos [2\pi f_{RF}(t - \tau_0 - \tau)]\} + \\
& \left. + 2 r_1 r_2 \{1 + m_I \cos [2\pi f_{RF}(t - \tau_0)]\}^{\frac{1}{2}} \cdot \right. \\
& \left. \cdot \{1 + m_I \cos [2\pi f_{RF}(t - \tau_0 - \tau)]\}^{\frac{1}{2}} \cdot \right. \\
& \cdot \mathcal{R}\varepsilon \left\{ \left[e^{j m_P \sin [2\pi f_{RF}(t - \tau_0)]} \cdot \right. \right. \\
& \left. \left. e^{-j m_P \sin [2\pi f_{RF}(t - \tau_0 - \tau)]} \right] e^{j 2kL} \right\} \Big) \qquad (2)
\end{aligned}
$$

where the property $\int_{S_{PD}} \overline{e}(x,y) \cdot \overline{e}^*(x,y) \, dS = 1$ has been exploited, and where the operator $\mathcal{R}\varepsilon \{...\}$ means that the real part of $\{...\}$ has to be considered.

With reference to the exponential functions inside the operator $\mathcal{R}\varepsilon \{...\}$ in Eq. (2), the trigonometric property $\sin(\zeta) - sin(\xi) = 2 \sin\left(\frac{\zeta - \xi}{2}\right) \cos\left(\frac{\zeta + \xi}{2}\right)$ is applied, and the relationship $e^{ju\cos(v)} = \sum_{n=-\infty}^{\infty} j^n J_n(u) e^{jmv}$ is exploited, where $J_n(u)$ is the Bessel function of first kind and of order n, and where in this case it is $u = 2 m_P \sin\left(2\pi f_{RF} \frac{\tau}{2}\right)$, $v = 2\pi f_{RF} \left[t - \left(\tau_0 + \frac{\tau}{2}\right) \right]$.

Some approximations are now introduced to Eq. (2). First of all, it is assumed that m_I is sufficiently smaller than unity (in the cases analyzed in this work, it is $m_I \leq 0.3$) so that an approximation to the first order can be applied to the square roots in Eq. (2). A similar assumption is taken for the quantity u, since commercial lasers exhibit typically $K_f \leq 200 \left[\frac{MHz}{mA}\right]$, and modulating currents with amplitude $I_{RF} < 10\, mA$ (corresponding to $P_{RF} \simeq 4\, dBm$) and frequencies f_{RF} lower than a few GHz have been here utilized. It can then be written $e^{ju\cos(v)} \simeq J_0(u) + 2jJ_1(u)\cos(v) \simeq 1 + ju\cos(v)$. Moreover, the products between m_I and u as well as the terms of order higher than one in $(r_1 \; r_2)$ are neglected.

After some simple derivations, the amplitudes of DC and RF components of the detected current (I_{DC} and I_{RF}, respectively), normalized with respect to $|E_0|^2$ can be expressed in the following form:

$$
\begin{aligned}
& \frac{I_{DC}}{|E_0|^2} = i_{DC} = \\
& = 1 + 2 r_1 r_2 \cos(2kL) = \\
& = i_{DC0} + \Delta i_{DC} \qquad (3)
\end{aligned}
$$

$$
\begin{aligned}
& \frac{I_{RF}}{|E_0|^2} = i_{RF} = \\
& = m_i + 2 r_1 r_2 \cos\left(2\pi f_{RF} \frac{\tau}{2}\right) \cdot \\
& \cdot \left\{ \left[m_i \cos\left(2\pi f_{RF} \frac{\tau}{2}\right) \right]^2 + \right. \\
& \left. \left[2 m_P \sin\left(2\pi f_{RF} \frac{\tau}{2}\right) \right]^2 \right\}^{1/2} \cdot \\
& \cdot \cos(2kL + \vartheta_{RF}) = \\
& = i_{RF0} + \Delta i_{RF} \qquad (4)
\end{aligned}
$$

with:

$$
\vartheta_{RF} = tg^{-1} \left[\frac{2 m_P}{m_I} tg\left(2\pi f_{RF} \frac{\tau}{2}\right) \right] \qquad (5)
$$

In both Eq. (3 and Eq. (4) it is possible to identify the contribution coming from the double reflection, which is the term multiplied by the two coefficients $r_1 r_2$.

2.3. Influence of temperature gradients

It is now assumed that the laser device undergoes time changes of the temperature T, as it happens typically in outdoor operation. Various consequences are determined by these changes. First of all, since it is $I_{th} = I_{th}(T)$, $\eta_0 = \eta_0(T)$ and $\eta_{RF} = \eta_{RF}(T)$, it will be $E_0 = E_0(T)$ and $m_I = m_I(T)$. Moreover, the index of refraction of the

fiber span will be influenced by the variation of T, leading to changes of β and eventually of τ_0. In response to monothonic variations of T, these quantities exhibit a monothonically varying behavior [15], [16]. The same monothonic behavior is then expected for I_{DC} and I_{RF}, and can be typically put into account at the design and/or post processing stages exploiting either *ad hoc* characterizations performed on the components utilized and/or the information given by the suppliers. In addition to this, the optical wavelength λ of the field emitted by the laser source will vary with T as $\lambda = \lambda_0 + \Delta\lambda(T)$, where λ_0 is the optical wavelength at the reference temperature T_0. Since it is $|\Delta\lambda(T)| << \lambda_0$, it is possible to write $k \simeq k_0 - k_0 \frac{\Delta\lambda(T)}{\lambda_0}$, with $k_0 = \frac{2\pi}{\lambda_0}$. With reference to this phenomenon, it is assumed that $\Delta\lambda(T)$ can be approximated in Taylor series truncated to the first order, taking $\Delta\lambda(T) \simeq \frac{d\,[\Delta\lambda]}{d\,T}(T - T_0) = \frac{d\,\lambda}{d\,T}(T - T_0)$.

This effect of the variation of T influences the terms Δi_{DC} and Δi_{RF} of Eq.s (3) and (4), but it does not lead in this case to monothonic variations of I_{DC} and I_{RF}. Indeed, the variation of λ affects the argument of the functions $\cos(2kL)$ and $\cos(2kL + \vartheta_{RF})$ of Eq.s (3) and (4), respectively. An oscillating behavior is then exhibited by these terms in correspondence to monothonic time variations of T. As an example, Fig. 3 shows in logarithmic scale simulated behaviors of i_{DC} and i_{RF} with respect to $\langle i_{DC}\rangle$ and $\langle i_{RF}\rangle$ (where the symbol $\langle\ldots\rangle$ means that the average value of $\ldots$ is taken), in a realistic case where the temperature T exhibits a decrease followed by a stationary and then by an increasing behavior.

It can be noticed that rippling behaviors result for $i_{DC}/\langle i_{DC}\rangle$ and $i_{RF}/\langle i_{RF}\rangle$ (see the thick dashed and thick continuous lines reported in Fig. 3, respectively) due to the double reflection described above, combined with the dependence $\frac{d\,[\Delta\lambda]}{d\,T}$. On the contrary, if only the monotonic dependencies mentioned at the beginning of the subsection were taken into account, the behaviors would be the ones of $i_{DC\,0}/\langle i_{DC}\rangle$ and $i_{RF\,0}/\langle i_{RF}\rangle$ which are represented in thin, dashed and thin, continuous lines, respectively, and do not exhibit any ripple, in contrast with the experimental evidence.

Another point to be noted is that, while the fluctuations of i_{DC} depend only on $\cos(2kL)$, as can be seen from Eq. (3), the fluctuations of i_{RF} depend on $\cos(2kL + \vartheta_{RF})$, as can be seen from Eq. (4). A phase displacement is then present between i_{DC} and i_{RF}, and can be appreciated in Fig. 4, where the behaviors of i_{DC} and i_{RF} are reported normalized respectively to the just defined quantities i_{DC0} and i_{RF0}.

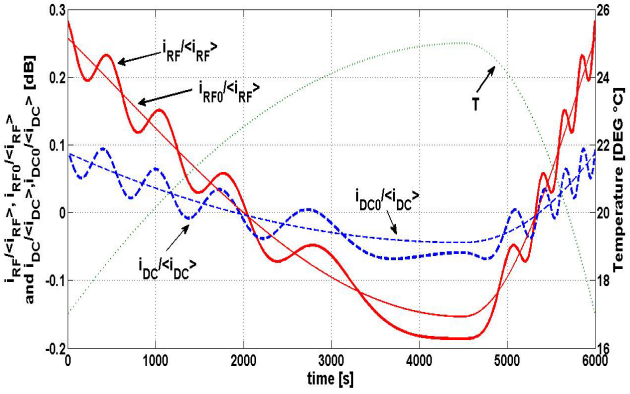

Figure 3: Example of simulated behavior in logarithmic scale of $i_{DC}/\langle i_{DC}\rangle$ (thick dashed line) and $i_{RF}/\langle i_{RF}\rangle$ in correspondence to varying values of the temperature T over time (dotted line). The rippling effect due to the undesired small reflections is superimposed to the expected behaviors $i_{DC\,0}/\langle i_{DC}\rangle$ and $i_{RF\,0}/\langle i_{RF}\rangle$ (thin dashed and continuous lines, respectively) that would result accounting only for the dependencies of I_{th}, η_0 and η_{RF} from T. See text for details.

With reference to Fig. 4, some points can be underlined. First of all, through the normalization performed, it is possible to focus the attention on the fluctuating behavior of the received currents, which is the phenomenon analyzed in this work. Moreover, unlike Fig. 3, where the variable T it is represented, in Fig. 4, the behavior of λ is reported,assuming a typical value of $\frac{d\,\lambda}{d\,T} = 0.1\left[\frac{nm}{^\circ C}\right]$, to stress the fact that the fluctuating behaviors are related to the time variation of the wavelength λ. Referring again to Fig. 4, note that in correspondence to the negative time slope of λ, the curve of $\frac{i_{DC}}{i_{DC_0}}$ leads the $\frac{i_{RF}}{i_{RF_0}}$ one, then, in correspondence of the stationary behavior of λ, the two curves are in phase, and finally, in correspondence to the positive time slope of λ, the curve of $\frac{i_{DC}}{i_{DC_0}}$ lags the $\frac{i_{RF}}{i_{RF0}}$ one. This is due to the fact that the change of sign in the time slope of $\Delta\lambda(T)$ is the equivalent of a change of sign in the phase displacement between the two curves. Note also that, due to the expression of ϑ_{RF} given by Eq. (5), this phase displacement is related to m_P, namely to the presence of the frequency chirp of the directly modulated laser.

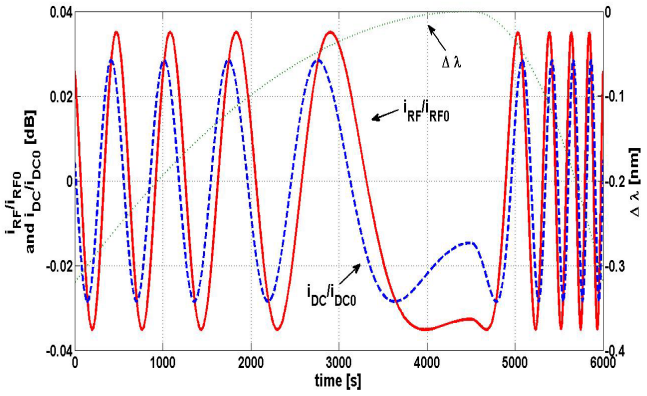

Figure 4: Simulated behavior in logarithmic scale of i_{DC}/i_{DC_0} (dashed line) and i_{RF}/i_{RF_0} (continuous line) in the same case of Fig. 3, in correspondence to varying values of the wavelength variation $\Delta\lambda = \lambda - \lambda_0$ over time (dotted line). See text for details.

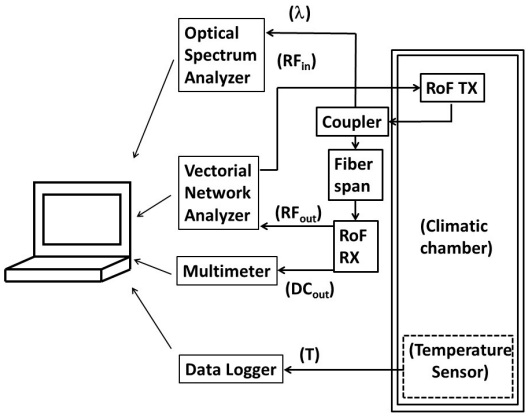

Figure 5: Setup utilized for the laboratory experiments.

3. Experimental results and discussion

3.1. Confirmation of the model developed

The laboratory activity was performed utilizing a setup like the one depicted in Fig. 5, where a RoF Tx emitting in the second optical window was connected through a fiber span to a RoF Rx based on a PIN photodiode.

The system was modulated by a RF tone through a Vectorial Network Analyzer (VNA). Through an optical coupler, a part of the optical power was sent to an Optical Spectrum Analyzer, in order to monitor in real time the value of the central wavelength of the laser emission spectrum. The RoF Tx was placed in a climatic chamber to emulate the temperature variation experienced in outdoor operation.

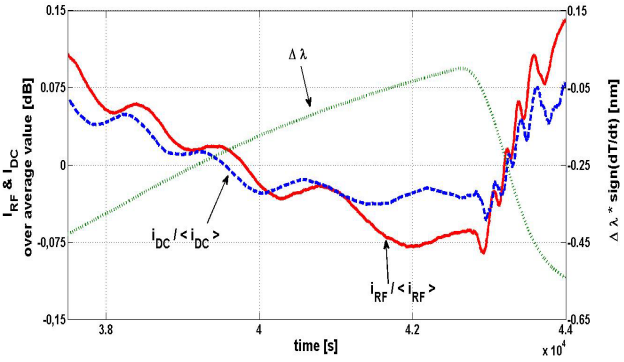

Figure 6: Measured behavior in dB of i_{DC} (dashed line) and i_{RF} (continuous line), referred to their respective average values, versus time. The values of $\Delta\lambda$ over time (dotted line) are represented as well. See text for details.

The frequencies of the RF tones were changed from $100MHz$ to $1GHz$, determining in all cases similar behaviors of the quantities analyzed. Without loss of generality, in the remainder we will refer to the value $f_{RF} = 600MHz$. For the initial tests, it was utilized a RoF link of the same kind of the ones utilized in the Northern Cross Radiotelescope which led to the results reported in Fig. 2. The RoF Tx was based on a directly modulated DFB laser which was experimentally characterized, confirming the linear dependence assumed for λ with respect to T, with $\frac{d\,\lambda}{d\,T} \simeq 0.1\left[\frac{nm}{^\circ C}\right]$. Moreover, in the range of temperature considered, it resulted possible to assume a linear dependence with respect to T also for i_{DC0} (which is proportional to the theoretical monothonic behavior of the emitted optical power P_0) and i_{RF0}, with $\frac{1}{\langle i_{DC0}\rangle}\frac{d\,i_{DC0}}{d\,T} \simeq -2\cdot 10^{-3}\left[\frac{1}{^\circ C}\right]$, $\frac{1}{\langle i_{RF0}\rangle}\frac{d\,i_{RF0}}{d\,T} \simeq -4\cdot 10^{-3}\left[\frac{1}{^\circ C}\right]$. The value of m_I in the different tests performed was always such that $0.05 \leq m_I \leq 0.3$. Since the phenomenon under investigation is to be ascribed to the RoF Tx alone, and is not influenced by the other components of the link, in particular, by the length of the SMF span, the RoF link was equipped with the only fiber span obtained from the connection of the RoF Tx pigtail to the RoF Rx one. Fig 6 reports measured behaviors of $i_{DC}/\langle i_{DC}\rangle$ and $i_{RF}/\langle i_{RF}\rangle$.

The RoF link was in this case modulated with $m_I = 0.27$. The fluctuating behaviors, predicted previously through Fig. 4, can be clearly appreciated, with reference to all the quantities considered. Note that, as predicted by the model, a phase displacement is observed between the rippling be-

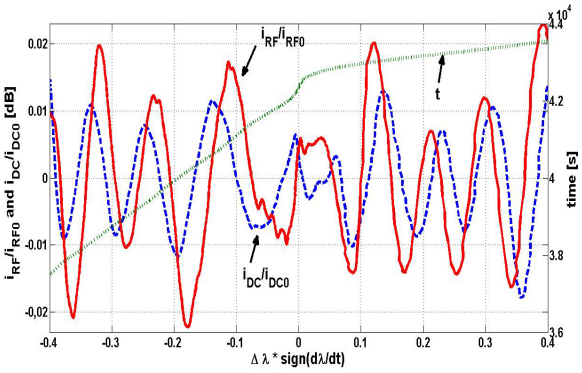

Figure 7: Observed behaviors of i_{DC}/i_{DC_0} (dashed line) and i_{RF}/i_{RF_0} (continuous line) as a function of $\Delta\lambda \cdot sign(d\lambda/dt)$. The corresponding values of the time t are also reported as a reference. See text for details.

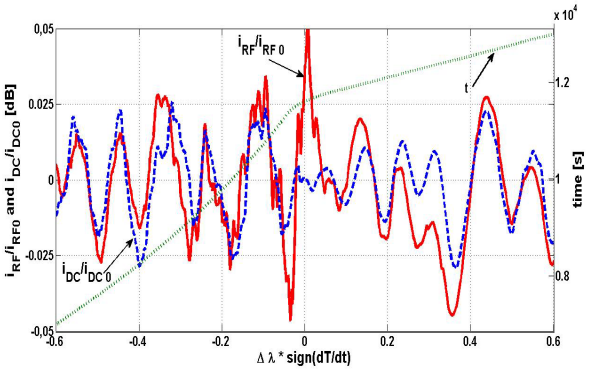

Figure 8: Observed behaviors of i_{DC}/i_{DC_0} (dashed line) and i_{RF}/i_{RF_0} (continuous line) as a function of $\Delta\lambda \cdot sign(d\lambda/dt)$, in the case when an external modulation in imposed to the RoF system through a Mach Zehnder Modulator with a chirp coefficient of a few MHz/mA. The corresponding values of the time t are also reported as a reference. See text for details.

haviors of DC and RF components of the detected current. This can be better appreciated in Fig. 7, where the behaviors of $\frac{i_{DC}}{i_{DC_0}}$ and $\frac{i_{RF}}{i_{RF_0}}$ are plotted in logarithmic scale.

Indeed, in Fig. 7 as the variable quantity in abscissa, instead of time t, it is used the instantaneous value of the wavelength variation $\Delta\lambda(t)$ multiplied by $sign\left(\frac{d\,\lambda}{d\,t}\right)$, so that the cases of downward and upward slope of λ can be distinguished. The reason is that the period of the ripples results to be the same in terms of λ variations, and this leads to a better appreciation of the phase displacement of the curves. On the contrary, reporting the behaviors in terms of time, the period of the fluctuations may be shorter or longer, in dependence of the speed of variation of λ (caused, in turn, by the speed of variation of T). The phase displacement shown in Fig. 7 is a further confirmation of the model developed in the previous section. Indeed, it can be appreciated that, in correspondence to a negative or a positive time slope of T, the curve of $\frac{i_{DC}}{i_{DC_0}}$ respectively leads or lags the $\frac{i_{RF}}{i_{RF_0}}$ one. The behaviors reported in Fig.s 6 and 7 could be correctly simulated by our modeling program, exploiting the above mentioned parameters of the components utilized, and assuming $r_1 r_2 = 0.9 * 10^{-3}$, $L = 3.9 * 10^{-3} m$.

To confirm that the phase displacement between $\frac{i_{DC}}{i_{DC_0}}$ and $\frac{i_{RF}}{i_{RF_0}}$ is due to the chirping effect of the directly modulated laser, a further experiment was performed. The RoF link was maintained in all its features, save for the fact that, instead of a direct modulation, an external modulation was applied to the optical field emitted by the Rof TX, which operated in Continuous Wave mode. The external modulation was performed through an electro-optic dual output integrated Mach Zehnder Modulator (MZM) from Corning OTI, whose adiabatic chirp coefficient was a few $\frac{MHz}{mA}$, much lower with respect to the adiabatic chirp coefficient of the laser utilized ($K_f \simeq 130\left[\frac{MHz}{mA}\right]$). The MZM was placed out of the climatic chamber, while the RoF Tx was placed inside. As can be appreciated in Fig. 8, the phase displacement between the two curves almost disappeared with respect to Fig. 7, confirming that, since it can be put $m_P \simeq 0$ in Eq. (4) and (5) , both Δi_{DC} and Δi_{RF} are proportional to $\cos(2kL)$.

After having validated the theoretical model proposed, an observation of practical interest is that, since a complete ripples cycle is observed every time the quantity $2k_0 L \frac{\Delta\lambda(T)}{\lambda_0}$ reaches the value 2π, with the typical values exhibited by the various quantities, it is enough to let the laser undergo a temperature variation of a few degrees centigrades to determine the amplitudes of the fluctuations of i_{DC}, i_{RF}, and consequently the effective values of the ripples.

3.2. Analysis of different kinds of lasers

Once the terms of the problem have been identified, it is necessary to determine a way to keep the problem itself under control. In the case of the SKA Design Study project, a mitigation of the undesired effect emerged *a posteriori* in the realization of the BEST-2 system, where the Northern Cross Radio Telescope was equipped with 32 distributed optical

links of the type studied in Section 3.1, carrying information of a given RF sky observation. Indeed, the laser sources of the various optical links exhibited slightly different values of the distance L, of the initial emission wavelength λ and of the initial optical field phase (which, considering only one link, was put to zero for simplicity in our model). This, added to the fact that the field experienced different group delays because of the different link lengths, resulted in a global reduction of the undesired rippling effect, when observations based on the interferometric technique had to be performed [19]. Indeed the post-processing is in this case based on the search of correlated behaviors, and this results in an effect of mutual cancellation when it comes to the fluctuating behaviors of the received signals.

This cannot be however regarded as a general solution. For example, talking about arrays, when, instead of interferometric observations, the technique of adaptive beamforming is utilized, a summation of the different received signals is performed at the postprocessing stage, and the mitigation effect cannot be guaranteed in this case. Moreover, in the applications where a single antenna is utilized, no mitigation effects can be expected.

In order to determine a general solution, valid for all the possible applications, a minimization of the backreflection effect, in the region where the coupling from the laser to the fiber is performed, is mandatory. Custom solutions can be realized to this purpose ([20], [21]) which can easily reach high level in terms of associated costs.

With the aim to minimize the undesired effect and at the same time avoid resorting to custom solutions, a series of tests has then been performed to analyze the presence of the phenomenon in different kinds of lasers sources commercially available,

Since the observed behavior is due to the laser source alone, the analysis has been performed with the same methodology both in the cases when the directly modulated laser source is inserted in a RoF TX or when it is housed in a plain package like the pigtailed coaxial one or the Transmitter Optical Sub Assembly (TOSA). The laser sources have been analyzed through the same measurement procedure depicted in Fig. 5, in which the fiber span consisted in the pigtails of the RoF Tx and of the RoF Rx.

In order to compare the performances of the different lasers, the standard deviation σ_{RF} has been considered, of the quantity $\frac{i_{RF}}{i_{RF_0}}$, expressed in logarithmic scale. Besides DFB lasers, also lasers of Fabry-Perot (FP) and Vertical Cavity Surface Emitting (VCSEL) type have been utilized, since they constitute a possible choice in the realization of the transmitter side of RoF systems [17] [18]. In these cases, the lower coherency, with respect to DFBs, does not allow to apply with sufficient approximation the mathematical model described in the previous section. The theoretical results can anyway still be utilized as a qualitative reference to interpret the experimental results obtained with FP lasers and VCSELs. Note also that one of the VCSELs considered was actually emitting at $\lambda = 850nm$. In this case the measurement setup has been the same, except for the fact that the fiber span consisted in a silica 62.5/125 multimode fiber. However, the performance of this laser source could be compared with the others, because also in this case a fiber span of a few meters was utilized, and the effects of multimodality did not impede to observe the effects of the optical backreflection.

Table 1 summarizes the results of the measurement performed. The levels of σ_{RF} have been classified as high, low and absent if $\sigma_{RF} \in [0.01, 0.03]dB$, $\sigma_{RF} \in [0.003, 0.009]dB$ and $\sigma_{RF} < 0.003dB$, respectively.

For each considered device, other data are included, like the possible presence of an optical isolator at the laser output or a qualitative comment on the cost. Some observations can be performed at this point. It can be noted that there is not a clear biunivocal correspondence between the level of σ_{RF} and the other illustrative parameters (type of laser considered, level of price, etc.). However, some reference relationships can be still identified among them. Firstly, it can be noted that all the lasers equipped with an optical isolator exibit tendentially (with exceptions given by laser numbered as 1 and 5 in Table 1) a low or absent level of σ_{RF}. Conversely, with the exception of the already cited laser n. 1 and 5, all the lasers which exhibit a high level of σ_{RF} are not equipped with an optical isolator. This tendential relationship can be logically expected, since the presence of this component reduces the backreflection effects at the laser−fiber coupling section. At the same time, it must be noted that all the lasers with optical isolator present in all instances a medium to high price. Among the lasers equipped with the optical isolator, the ones which in addition feature a thermostabilization apparatus guarantee with no exception a low level of σ_{RF}. This can be explained by the fact that in this case, the problem studied is tackled also up-

n.	Laser model	Laser type	Other information	Level of σ_{RF}	Presence of optical isolator	Laser price level
1	Sumitomo SLT 4260-XS/TM1 L7YFT3108	DFB, 1310nm	Pigtailed	High	Yes	Medium
2	Sichuan JiuZhou JZD13P	DFB, 1310nm	Pigtailed	High	No	Low
3	Sichuan JiuZhou JZD15P	DFB, 1550nm	Pigtailed	High	No	Low
4	Finisar HFE4192-58X	VCSEL 850 nm	TOSA	High	No	Low
5	Mitsubishi FU450SDF FL41M13B	DFB, 1310nm	Pigtailed	High	Yes	Medium
6	Eudina FLD3F7CZ-N3 ORO1649	DFB 1310nm	Pigtailed, Thermo stabilized	Low	Yes	High
7	Sumitomo SLT S412 DB-F370	DFB 1310nm	Pigtailed, Thermo stabilized	Low	Yes	High
8	K2 Optronics ECQA-100 330-10-FA	DFB 1310nm	Pigtailed, Thermo stabilized	Low	Yes	High
9	Eudina FLD5F7CZ IW06505	DFB 1310nm	Pigtailed	Low	Yes	Medium
10	Mitsubishi FU-450SDF FL41M23B	DFB 1310nm	Pigtailed	Low	Yes	Medium
11	Avago AFBR-1310Z	FP 1310nm	Pigtailed	Absent	No	High
12	Vertilas V260739	VCSEL 1310nm	Pigtailed	Absent	No	High
13	Sumitomo STV3ZE0-QS/R	DFB 1310nm	Pigtailed	Absent	Yes	High
14	Sumitomo STV3ZF0-QS/R	DFB 1310nm	Pigtailed	Absent	Yes	High
15	Sumitomo STP3ZE0-QS	DFB 1310nm	Pigtailed	Absent	Yes	High

Table 1: Comparison of the standard deviations σ_{RF} of the quantity $\frac{i_{RF}}{i_{RF0}}$ for different laser sources due to the rippling behavior described in this work. Other descriptive information for each laser are reported. See text for details.

stream, impeding that the temperature variations of the environment can have sensible impact on the value of the emitted wavelength λ. The adoption of a thermo-stabilized laser source could then constitute a solution to the problem, but, again, at the expense of an increase in the cost of the device. Focusing now the attention on the lasers which exhibit an absent value of σ_{RF}, it can be observed that all of them exhibit a high cost, and three of them (lasers 12-14 of Table 1) are equipped with an optical isolator. The remaining two lasers, which are not equipped with an optical isolator, are respectively of FP type (laser n. 11), and VCSEL type (laser n. 12). Qualitatively speaking, the lower degree of coherence of the emitted optical power with respect to DFB lasers could possibly play a role in obtaining this result, since the interference effect caused by the backreflection would be inhibited. However, this reason cannot be the only one, since laser n.4 which is also of VCSEL type (but of lower price level), exhibits a high level of σ_{RF}. Translating into some final observation the comparison performed, it must be underlined that other laser parameters, like for example the Spurious Free Dynamic Range, must be taken into account, in addition to the ones considered, to perform an optimal choice. The final decision will then depend each time on the acceptable compromise among the needs of the considered application. However, regarding the fluctuating behavior examined in this work, it can be noted that, the fact that its presence or absence is not strictly related to a particular kind of laser determines positive consequences. One of them is that VCSEL sources, which are today particularly interesting, due to their low power consumption levels, can be found among those ones where this undesired phenomenon is absent.

4. Conclusions

Undesired fluctuating behaviors of the received optical power and of the RF gain in short-range analog Radio over Fibre links have been experimentally measured and theoretically explained. These behaviors, whose impact can be evaluated in a simple fashion, are due to the combined effect of temperature variation of the laser device and optical back reflection generated in the region between laser output and fibre input section. Through a measurement campaign which analyzed different laser types, it has been shown that the phenomenon can appear also when an optical isolator is introduced downstream of the laser output, or conversely, can be negligible in laser samples unprovided of such component. Through an appropriate pondering of the laser characteristics required by the application envisaged, it is possible to perform choices which minimize this behavior, and preserve at the same time cost effectiveness.

Acknowledgements

The authors thank Prof. Stefano Selleri of University of Parma for helpful discussions. Sponsorship from italian Ministry of University and Research (MIUR) is acknowledged as well.

References

[1] J. Capmany and D. Novak, "Microwave photonics combines two worlds", Nature Photonics, 1, pp. 319-330 (2007)

[2] J. Beas, G. Castanon, I. Aldaya, A. Aragon-Zavala, G. Campuzano, "Millimeter-Wave Frequency Radio over Fiber Systems: A Survey", IEEE Communications Surveys and Tutorials, Early access Article

[3] V. J. Urick, "Long-haul analog links tutorial", Optical Fiber Communication (OFC), San Diego, CA, 2010, pp. 1 - 39

[4] J. C.Velzquez, J. C. Montero, J. H. Rodrguez, R. Garduno, "Improved Analog Optical Fiber Link for Signal Measuring in a High Power Testing Facility," International Journal of Mathematics and Computers in Simulation, 1, pp. 40-45 (2007)

[5] S. Kingsley, B. Tian, S. Sriram, "Analog Fiber Optic Link for EMC emission testing." Available at http://www.srico.com/files/Item%2099%20article.pdf

[6] S. Montebugnoli, M. Boschi, F. Perini, P. Faccin, G. Brunori, E. Pirazzini, "Large antenna array remoting using radio-over-fiber techniques for radio astronomical application", Microwave and Optical Technology Letters 46, Issue 1, pap. 4854, (2005)

[7] E. Ackerman, C. Cox, J. Dreher, M. Davis, D. DeBoer, "Fiber-optic antenna remoting for radioastronomy applications", XXVII General Assembly of the International Union of Radio Science, Maastricht, The Netherlands, pp. 1-4, 2004

[8] H. Iwamura, S. Hayashi, and H. Iwasaki, "A compact Optical Isolator using a Y3Fe5O12 crystal for near-infrared radiation," Optical and Quantume Electronics, 10, pp. 393-398, 1978

[9] M. Labudovic and J. Li, "Modeling of TE cooling of pump lasers", IEEE Transactions on Components and Packaging Technologies, 27, pp. 724-730, 2004

[10] International Effort named "Square Kilometre Array" (https://www.skatelescope.org/project/)

[11] S. Montebugnoli, G. Bianchi, J. Monari, G. Naldi, F. Perini, M. Schiaffino, "BEST: Basic Element for SKA Training", Proceedings of the SKADS Conference Wide Field Science and Technology for the Square Kilometre Array, Chateau de Limelette, Belgium, 3-6 November 2009

[12] S. Montebugnoli,, G. Bianchi, C. Bortolotti, A. Cattani, F. Ghelfi, A. Maccaferri, F. Perini, J. Roda, M. Roma, G. Zacchiroli, L. Zoni,, "Re-instrumentation of the northern cross radio telescope for a SKA cylindrical concentrator based test bed," 34th European Microwave Conference, 2004., vol.3, no., pp.1537,1540

[13] K. Peterman and G. Arnold, "Noise and distortion characteristics of semiconductor lasers in optical fiber communication systems," IEEE Transactions on Microwave Theory and Techniques, 30, pp. 389401, (1982)

[14] G. Alcaro, D. Visani, L. Tarlazzi, P. Faccin, G. Tartarini, "Distortion Mechanisms Originating from Modal Noise in Radio over Multimode Fiber Links," IEEE Transactions on Microwave Theory and Techniques, 60, pp. 185-194 (2012)

[15] M. Yano, H. Nishi, and M. Takusagawa, "Temperature characteristics of threshold current in InGaAsP/inP doubleheterostructure lasers," Journal of Applied Physics 51, 4022-4028 (1980)

[16] D. F. Zaitsev, "Temperature drift of modulation characteristics in semiconductor lasers," IEE Proceedings Journal on Optoelectronics, 140, pp 227-231 (1993)

[17] D, Visani, F.Sorci, P. Faccin, G. Tartarini, "Comeback of Fabry-Perot RoMMF Transmitters for Improved LTE Signal Distribution," IEEE International Topical Meeting on Microwave Photonics (MWP) 2012 , Norwijk, The Netherlands

[18] R. Beresford, "ASKAP Photonic Requirements", Microwave Photonics 2008, Gold Coast, Qld, Sep. 29-Oct 1 2008, pp. 62-65

[19] F. Perini, "Analogue optical links experiences in the framework of the SKA/BEST activities", Proceedings of the SKADS Conference Wide Field Science and Technology for the Square Kilometre Array, Chateau de Limelette, Belgium, 3-6 November 2009

[20] S. K. Mondal, F. G. Shi, "Optimization of fiber-laser coupling with respect to both the coupling efficiency and carrier-to-noise ratio: a novel design" 52nd IEEE Electronic Components and Technology Conference, San Diago, CA, 31-May 2002

[21] OZ Optics LTD, "Laser to Fiber Source Couplers" Application Note, available at http://www.ozoptics.com/ALLNEW_PDF/APN0004.pdf